



# Laser-Assisted Fabrication of Nanostructured Substrate Supported Electrodes for Highly Active Supercapacitors

Mamoon Asghar<sup>1</sup>, Syedah Afsheen Zahra<sup>1</sup>, Zarah Khan<sup>1</sup>, Momina Ahmed<sup>1</sup>, Farheen Nasir<sup>2</sup>, Mudassir Iqbal<sup>1,3</sup>, Mohammad Ali Mohammad<sup>2\*</sup>, Asif Mahmood<sup>4\*</sup>, Deji Akinwande<sup>5</sup> and Syed Rizwan<sup>1\*</sup>

<sup>1</sup> Physics Characterization and Simulations Lab (PCSL), Department of Physics, School of Natural Sciences (SNS), National University of Sciences and Technology (NUST), Islamabad, Pakistan, <sup>2</sup> School of Chemical and Materials Engineering (SCME), National University of Sciences and Technology (NUST), Islamabad, Pakistan, <sup>3</sup> Department of Chemistry, School of Natural Sciences (SNS), National University of Sciences and Technology (NUST), Islamabad, Pakistan, <sup>4</sup> School of Chemical and Biomolecular Engineering, The University of Sydney, Sydney, NSW, Australia, <sup>5</sup> Microelectronics Research Center, The University of Texas at Austin, Austin, TX, United States

## OPEN ACCESS

### Edited by:

Mohammad Islam,  
King Saud University, Saudi Arabia

### Reviewed by:

Amir Habib,  
University of Hafr Al Batin,  
Saudi Arabia  
Wei Kong Pang,  
University of Wollongong, Australia

### \*Correspondence:

Syed Rizwan  
syedrizwan@sns.nust.edu.pk;  
syedrizwanh83@gmail.com  
Asif Mahmood  
asif.mahmood@sydney.edu.au;  
asifmahmoodnust@yahoo.com  
Mohammad Ali Mohammad  
dr.ali@scme.nust.edu.pk

### Specialty section:

This article was submitted to  
Energy Materials,  
a section of the journal  
Frontiers in Materials

**Received:** 31 March 2020

**Accepted:** 15 May 2020

**Published:** 22 July 2020

### Citation:

Asghar M, Zahra SA, Khan Z, Ahmed M, Nasir F, Iqbal M, Mohammad MA, Mahmood A, Akinwande D and Rizwan S (2020) Laser-Assisted Fabrication of Nanostructured Substrate Supported Electrodes for Highly Active Supercapacitors. *Front. Mater.* 7:179. doi: 10.3389/fmats.2020.00179

Supercapacitors (SCs) have attracted great attention as renewable energy storage devices due to their high power densities and cost effectiveness. In this work, a one-step method is reported to fabricate the laser scribed SC using laser reduced Polyimide (LRPI) electrodes as a substrate. An Iono-gel polymer electrolyte based on polyvinyl alcohol, potassium hydroxide and 1-Butyl-3-methyl imidazolium Bromide ([Bmim]Br) was utilized because of its wider voltage window, good ionic conductivity and better adhesion with electrode material. The assembled device exhibited an excellent specific capacitance of 2.19 mFcm<sup>-2</sup> at a maximum current density of 0.263 mAcm<sup>-2</sup>. The energy density is measured to be 1.21 μWhcm<sup>-2</sup>, which is much higher than a usual capacitor. Given these electrochemical properties, a cost-effective one-step method and scalable approach provides a strategy to fabricate lightweight, stretchable and flexible supercapacitors for future microscale energy storage devices i.e., flexible displays, electrical sensors and wearable electronics.

**Keywords:** supercapacitor, polyimide, reduced polyimide, ionic liquid, laser processing, laser reduction

## INTRODUCTION

Economical, efficient, and clean energy storage technologies are urgently needed to handle the expeditiously exacerbated intermittence of renewable energies into the grid. The exigency of efficient, compact and environmentally friendly storage systems impels the development of ultracapacitors and batteries bearing high energy and power densities.

Electrochemical energy storage devices such as electrochemical batteries, supercapacitors (SCs) and fuel cells, etc. have received immense attention recently because of large scale applications, from portable electronic devices to large electric vehicles. Among these devices, SCs have shown promising applications for the quick generation of energy for startup applications, as well as for where burst-mode power is required. SCs store electric charge by the formation of an electrical double layer formed at electrode-electrolyte interface under potential gradient, which diffuses quickly upon potential inversion to deliver quick energy and take advantage of a high surface area,

high power density, low energy density, fast charging rate, and excellent cyclic stability (Winter and Brodd, 2009). Since charge storage in electrochemical double layer SCs is a surface-based phenomenon, the surface area of the electrodes, pore size distribution, the electrode/electrolyte interface, and electrical conductivity become very important. However, their performance is largely affected by poor contact between the electrode and current collector as well as structural degradation (Mahmood et al., 2016). Continuous proliferation of supercapacitors in hybrid and flexible energy storage devices requires an upsurge of power and energy density. Hence, developing new electrode chemistries which can exhibit superior capacitive performances without structural degradation is of prime interest.

Carbon-based electrodes have found significant interest in SCs because of their large surface area, elevated conductivity, and greater porosity. The carbon-based electrodes have been tailored in a number of ways to improve their capacitive performances, such as tuning of morphology to obtain layered, porous, 1-dimensional (1D), 2D, 3D nanostructures etc. (Tabassum et al., 2018). Designing different morphologies improves electrode/electrolyte contact, thus improving overall surface charge storage. Generally, the carbon-based electrode materials are prepared in bulk prior to loading to a current collector, which used dead mass in the form of binder and active carbon, resulting in relatively lower capacitance. Very recently, the developments of binder-free electrode chemistries have gained attention because of the possibility of direct utilization as an electrode without any further modification. Various binder-free electrode chemistries have been investigated, including a carbon nanotube (CNT) sponge, carbon fiber paper, carbon cloth, etc. However, these materials must be loaded onto the current collector for device fabrication, which again affects the efficient charge transfer from the electrode material to the current collector, resulting in poor capacitive charge storage capability (Mahmood et al., 2015). Thus, new electrode chemistries where partial *in-situ* surface conversion can activate the surface for enhanced charge storage could be a possible solution, where the converted surface will provide active sites for enhanced charge storage while the boon contact between active surface and the intact substrate will provide efficient charge transfer to boost the capacitance. Laser Induce graphene via laser lithiation has proven to be a promising material for the fabrication of electrodes for supercapacitors (Lin et al., 2014). The capacitance of these electrodes depends on various factors, including substrate material, surface area, laser power, and type of electrolyte (Malik et al., 2018).

In this work, we report a one-step method to fabricate laser-assisted reduced Polyimide (LRPI) electrodes where the surface of Polyimide (PI) is partially converted to graphitic carbon by laser irradiation. A PI sheet of average thickness of  $\sim 200 \mu\text{m}$  was exposed to a diode laser for the fabrication of SC electrodes (Huang et al., 2018). The SC device fabricated using LRPI as an active *in-situ* converted electrode and PVA-KOH-1-Butyl-3-Methylimidazolium Bromide ([Bmim]Br) electrode exhibited an excellent areal capacity of  $2.19 \text{ mFcm}^{-2}$  at a maximum current density of  $0.59 \mu\text{Acm}^{-2}$ . The dependence of capacitance on

various parameters such as the scan rate, size, geometry of electrodes, and laser intensity is reported. This one-step cost-effective synthesis technique will be vastly significant for the refashioning of flexible high energy density SC devices.

## EXPERIMENTATION

The LRPI electrodes were synthesized by using  $1 \text{ cm}^2$  PI as a precursor and a laser scribed process was used to reduce the PI into a conductive LRPI electrode. The laser reduces the non-conductive polyimide sheet to a conductive form of carbon similar to laser-induced graphene (LIG), where surface carbon provided active sites for charge storage. A computer-controlled laser engraver of wavelength  $\sim 450 \text{ nm}$  and pre-optimized laser power of  $\sim 164 \text{ mW}$  was used to reduce a PI sheet of area  $1 \times 1 \text{ cm}$ . All LRPI samples were fabricated at a fixed laser power of  $164 \text{ mW}$  with a beam diameter of  $\sim 70 \mu\text{m}$ . The laser setup consisted of two stepper motors that move in the 2D X-Y direction.

The LRPI electrodes having an area of  $1 \text{ cm}^2$  were assembled into an SC device using a PVA-KOH-([Bmim]Br) as an electrolyte and a separator. The Iono-gel electrolyte was prepared by mixing  $7 \text{ mg}$  of PVA and  $10 \text{ mg}$  of KOH in  $10 \text{ ml}$  deionized water under sonication at  $80^\circ\text{C}$  for  $1 \text{ h}$ . The gel-like material formed was cooled up to  $30^\circ\text{C}$ , which resulted in the formation of PVA-KOH-([Bmim]Br) electrolyte. To ensure the diffusion of ions, Iono-gel was applied to the electrodes of the device for  $1 \text{ h}$  prior to measurements.

## CHARACTERIZATION

The structural characterization of LRPI sheets was carried out by XRD using D8 Discover Diffractometer (Bruker ASX, Germany) utilizing  $\text{Cu K}\alpha$  as an X-ray source. Scanning electron microscope JSM-6490A was used for morphological analysis. Fourier Transform infra-red Spectroscopy was carried out using Bruker Alpha. The working of the device was checked via Cyclic voltammetry and Galvanostatic charge/discharge electrochemical measurements. Electrochemical testing for supercapacitor devices was performed on an electrochemical workstation. EC-lab software and ECI workstation have been used for measuring electrochemical properties of the device. Cyclic voltammetry was executed at a scan rate of  $20$  to  $100 \text{ mV/S}$  over a voltage window of  $-2$  to  $+2 \text{ V}$ . The following equation (Liu et al., 2015), was used to calculate the specific areal capacitance of SC from charge/discharge curves:

$$C_{\text{device}} = \frac{I}{\frac{dv}{dt}} \quad (1)$$

In Equation (1)  $I$  is the average discharge current and  $\frac{dv}{dt}$  is the slope of Galvano static discharge curves. Areal capacitance was determined by the following equation:

$$C = \frac{1}{2 \times s \times (v_f - v_i) \times \frac{dv}{dt}} \int_{v_i}^{v_f} I(V)dv \quad (2)$$

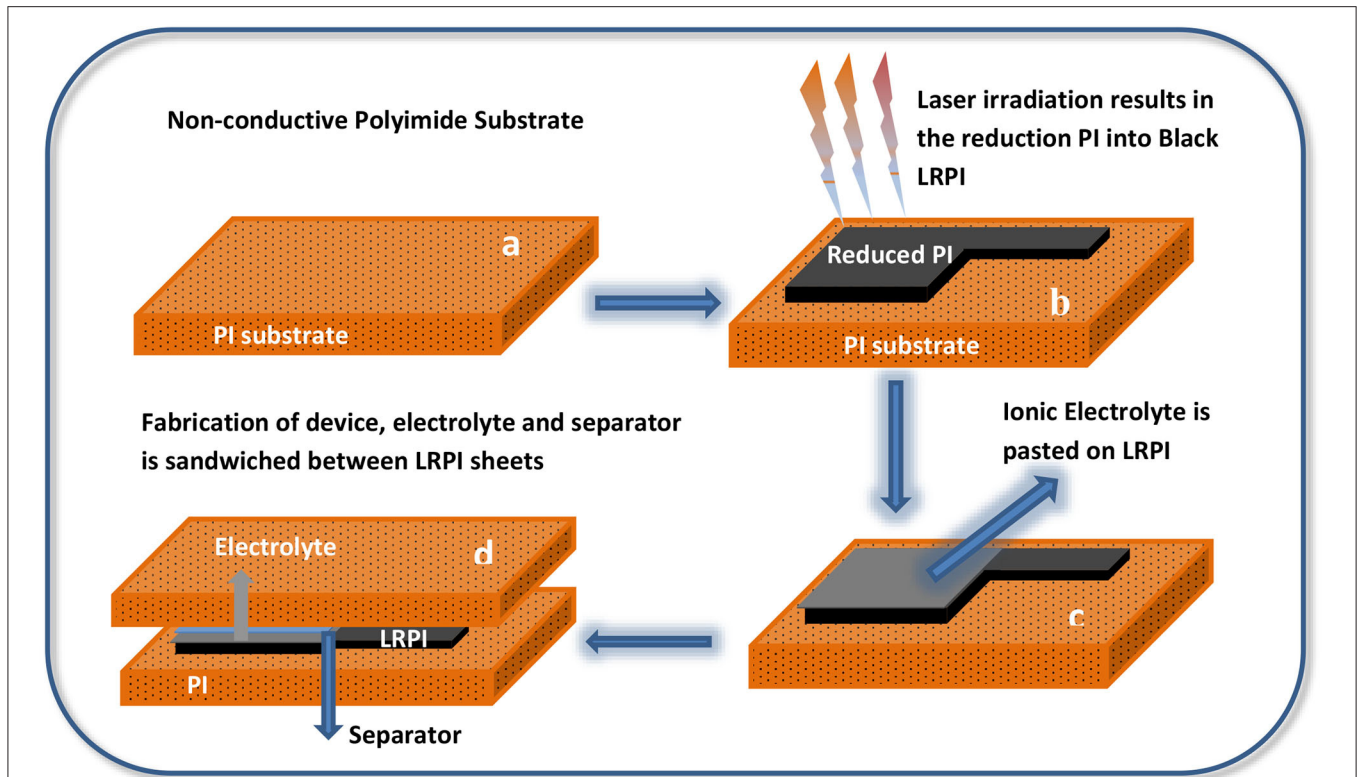


**FIGURE 1 | (a-d)** Schematic Diagrams showing fabrication steps of supercapacitor (b) shows image of PI and LRPI material which clearly shows that the PI material surface is altered after laser irradiation. (c) Ionic electrolyte is pasted on the reduced part of PI sheet to fabricate an electrode. (d) Separator is sandwiched between two electrodes to make an EDLC.

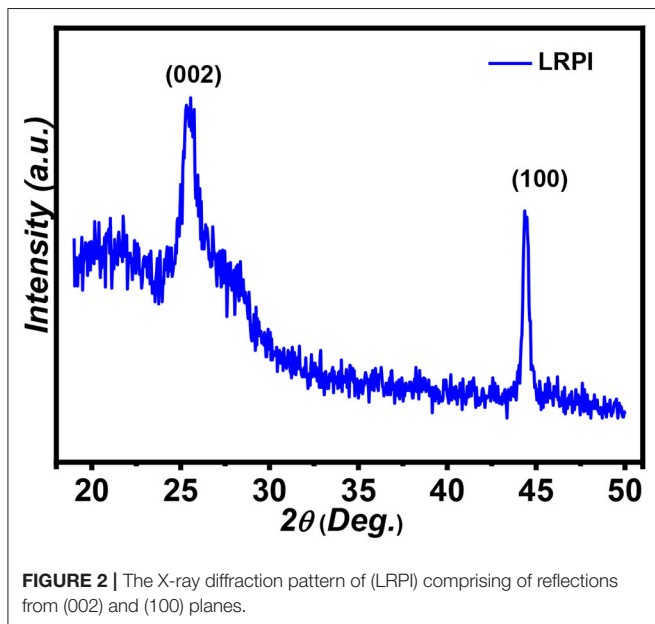


**FIGURE 2 |** The X-ray diffraction pattern of (LRPI) comprising of reflections from (002) and (100) planes.

Where  $C$  is the areal capacitance of LRPI and is measured in  $\text{mFcm}^{-2}$ ,  $s$  is the specific area of the electrodes ( $1 \text{ cm}^2$  in our case),  $v_f$  and  $v_i$  are the final and initial voltages (in Volts), and

$dv/dt$  is the scan rate (in  $\text{mV/s}$ ). The specific areal energy density  $E_A$  ( $\mu\text{Whcm}^{-2}$ ) and a real power density  $P_A$  ( $\mu\text{Wcm}^{-2}$ ) were calculated by the following equations (Hulicova and Puziy, 2009):

$$E = \frac{1}{2} \times C \times (\Delta V)^2 \times \frac{1}{3,600} \tag{3}$$

$$P_A = \frac{E_A}{t} \times 3,600 \tag{4}$$

$v\Delta V = V_{\text{max}} - V_{\text{drop}}$  is the discharge voltage range of SC.

## RESULTS AND DISCUSSION

Laser-scribing is a photothermal process which has been utilized to reduce polymers to obtain conductive carbon materials (Xin et al., 2017). A short wavelength (450 nm) laser pulse was used for *in-situ* conversion of PI into graphitic carbon to obtain LRPI as shown in **Figure 1**. The resulting LRPI material exhibits good electrical conductivity, increased porosity and high surface area. The reduced polyimide electrode has a porous surface and its conductive properties are between graphene and reduced graphene oxide (Malik et al., 2018). The alteration of the surface morphology of PI and LRPI is clearly visible and can be seen in **Figure 1** as real orange

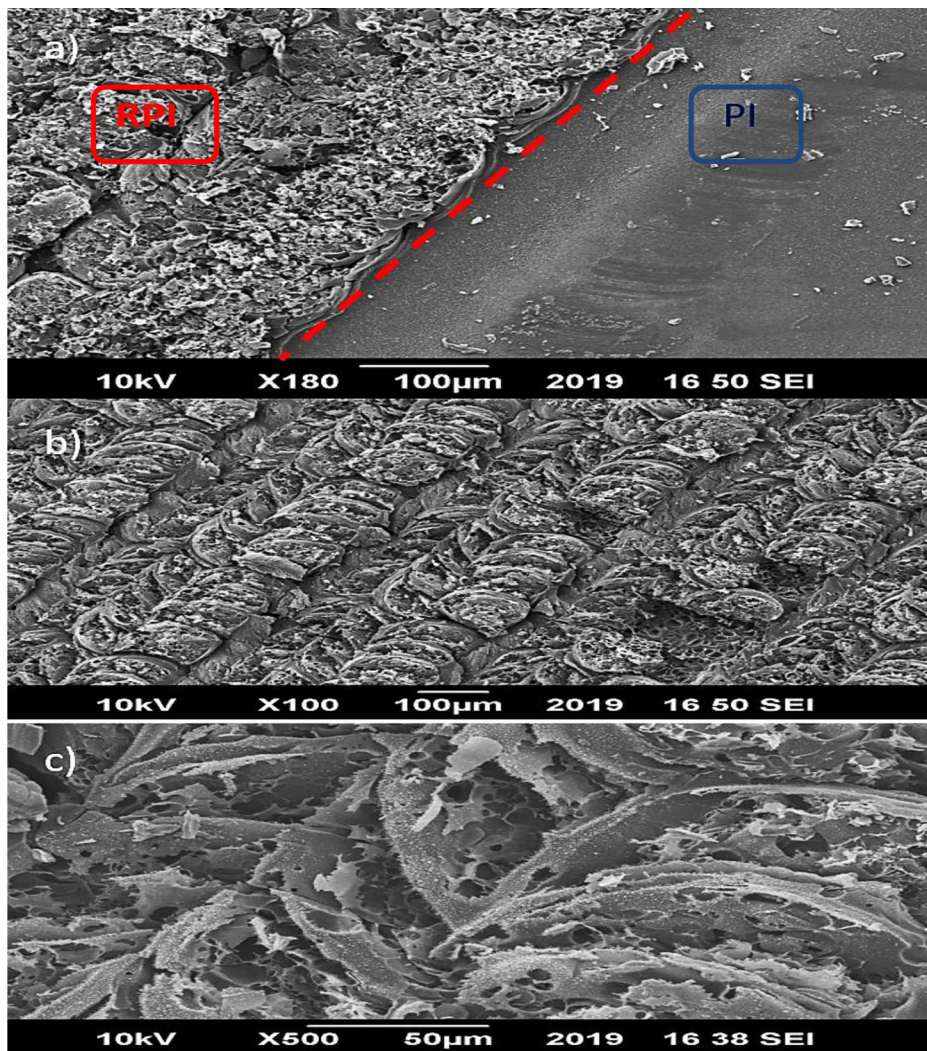


**FIGURE 3 |** (a) SEM image of irradiated PI at 164 mW laser power. The area on the right-hand side of the red dotted line represents the nonirradiated PI and the area on the left side of the dotted line represents the LRPI region. (b) Rough surface area of LRPI on top of PI substrate is shown as a result of laser irradiation. (c) Highly magnified image showing meso-macropores on the walls of LRPI and interconnection of carbon flakes with each other.

PI sheet is converted into black LRPI material due to laser ablation.

The Oxidation process in PI material gradually increases with the increase of laser power. Due to the high temperature of the laser beam the oxygen and nitrogen atoms will be liberated from PI material, leaving behind aromatic graphitic LRPI content. Thus, high laser power leads to high graphitization that increases the carbon content in LRPI.

The XRD pattern of laser reduced polyimide sheet obtained from commercially purchased PI sheet is shown in **Figure 2**. A sharp peak pivoted at  $2\theta = 25.44^\circ$  indicating an interlayer spacing of  $\sim 3.4 \text{ \AA}$  between the (002) planes, correlated to laser induced graphene like structures with high degrees of graphitization. The increased interlayer spacing is a result of defects produced on hexagonal graphene layers. A low intensity

peak at  $2\theta = 44^\circ$  represents the signature of reduction peak of PI into graphene-like LRPI material. This peak is reflection from (100) planes which is associated with the in-plane structure of LIG. The phenomenon of laser induced graphitization is attributed to the presence of repetitive aromatic and amide units in PI (Faghih and Ashouri, 2013; Lin et al., 2014; Tabassum et al., 2017).

Equations (5) and (6) are used to calculate the crystalline size along c axis ( $L_c$ ) and domain size along a axis ( $L_a$ ).

$$L_c = \frac{0.89\lambda}{B_{1/2}(2\Theta)\text{Cos}\Theta} \tag{5}$$

$$L_a = \frac{1.84\lambda}{B_{1/2}(2\Theta)\text{Cos}\Theta} \tag{6}$$

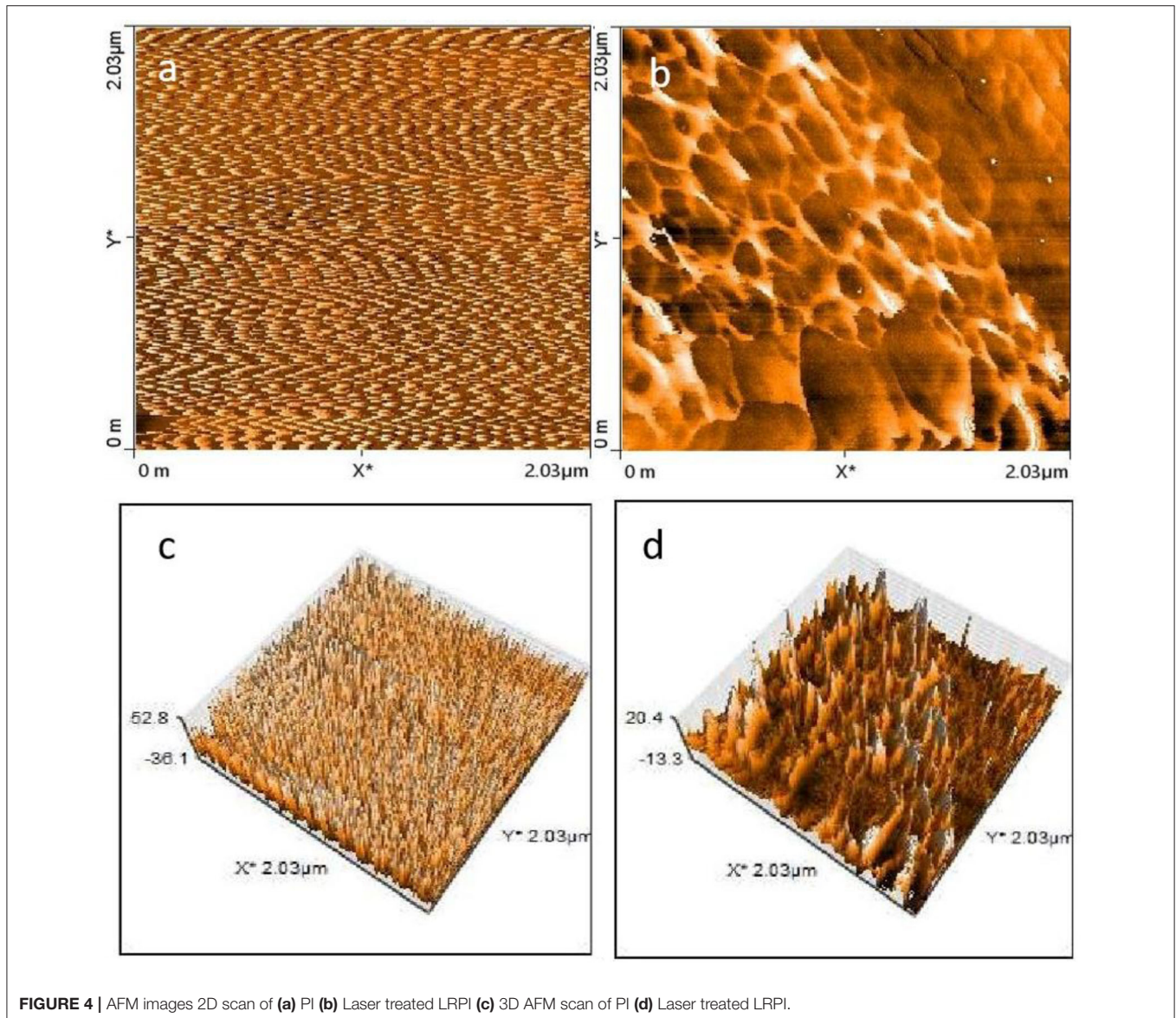


**FIGURE 4** | AFM images 2D scan of (a) PI (b) Laser treated LRPI (c) 3D AFM scan of PI (d) Laser treated LRPI.

Where

$B_{1/2}$  (radians) is the FWHM for peak (002) and  $\lambda = 1.544$  (Cu  $k_{\alpha}$  source of XRD).

$L_c$  and  $L_a$  are found to be 1.47 and 3.46 nm, respectively. This extended  $L_c$  is characteristic of LIG (Rathinam et al., 2017).

In **Figure 3a** non-irradiated plane area of PI material is distinguished with a red dotted line and the area beside the red dotted line corresponds to LRPI region. This figure indicates the impact of laser beam on PI sheet. Laser beam is capable of changes to the composition and the morphology of the material by cessation of volatile C-N, C-O-C, and C = O bonds, resulting in more carbon content as compared to unprocessed PI sheet, due to high temperature which results in a decrease of nitrogen and oxygen contents in PI (Zhu et al., 2011). Nitrogen and oxygen atoms in PI material would be released in the form of gases due to photothermal activity induced by laser (Romero et al.,

2018). The resulting content is converted into porous carbon material as can be seen in **Figure 3a**. The irradiated region in **Figure 3b** represents LRPI material on the top of PI sheet. This rough surface provides good adhesion with the electrolyte and thus contributes to enhanced diffusion which would result in an improved capacitance. **Figure 3c** shows the magnified SEM image of laser scribed cross-sectional area of LRPI material which shows the meso- micropores on the surface and also the strong interconnections of carbon flakes with each other. This figure shows that the carbon flakes are formed as a result of laser ablation, and are arranged in aromatic graphitic structure giving rise to graphitic content (Lin et al., 2012). This honeycomb structure is very advantageous for storage purposes, providing greater surface area and good adhesion. The layered flakes render the high porosity and provide active surfaces for the diffusion of electrolytes over the surface of active material. So the process

of facilitated diffusion is enhanced as a result of photothermal ablation of PI, resulting in LRPI porous layered flakes.

The surface morphology of PI and LRPI was further investigated using AFM with a resolution of  $\sim 1$  nm. The AFM was operated on the tapping mode due to smaller amplitude of

cantilever oscillations and fewer damages to the soft samples. **Figures 4a,b** represents the 2D scan of PI and LRPI respectively, while in image (**Figures 4c,d**) a 3D scan is shown.

The surface study reveals the compactness of PI film, the surface is smoother as compared to LRPI while presence of islands over LRPI surface is dominant, showing an overall increase in surface roughness which can be attributed to the laser treatment and subsequent conversion of polymer to graphitic carbon. After irradiation with laser, an increase in bump intensity is observed. This is due to an attack of high energy photons on the valance bonds of polymer, forming cleavage and crosslinking. A homogeneous layer is formed over the surface of PI, which is attributed to the degradation of PI to lower molecular weight species and carbon particles. It is quite clear that the surface roughness of LRPI is greater than the pristine PI which is consistent with surface topology results. The rough graphene-like surface plays a vital role in adhesion of electrolyte and formation double layer, thus enhancing the capacitive performance of a full device.

FTIR spectra were recorded to study the type of bonding in PI and LRPI material as shown in **Figure 5**. Laser irradiation causes a high temperature which leads to a breaking of bonds between Carbon, oxygen (C = O) and Nitrogen, Carbon (N-C). Change in the PI and LRPI peak indicate the stretching and bending of carbon, nitrogen and oxygen bonds at different frequency regions. Different types of stretching vibrations of the C-N bond

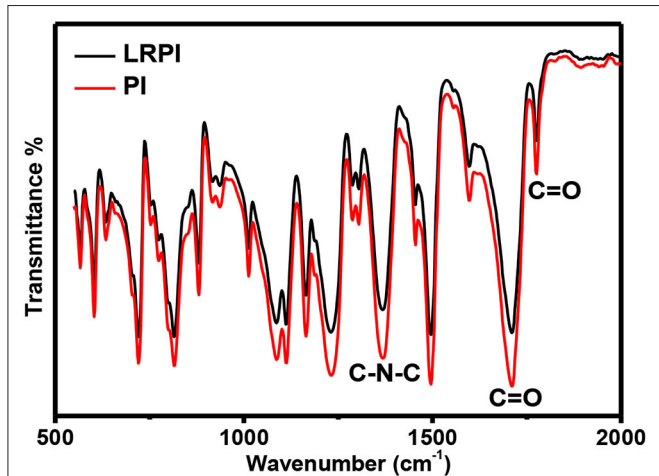


**FIGURE 5** | Comparison of PI and LRPI region from FTIR spectra using pre-optimized 164 mW laser power.

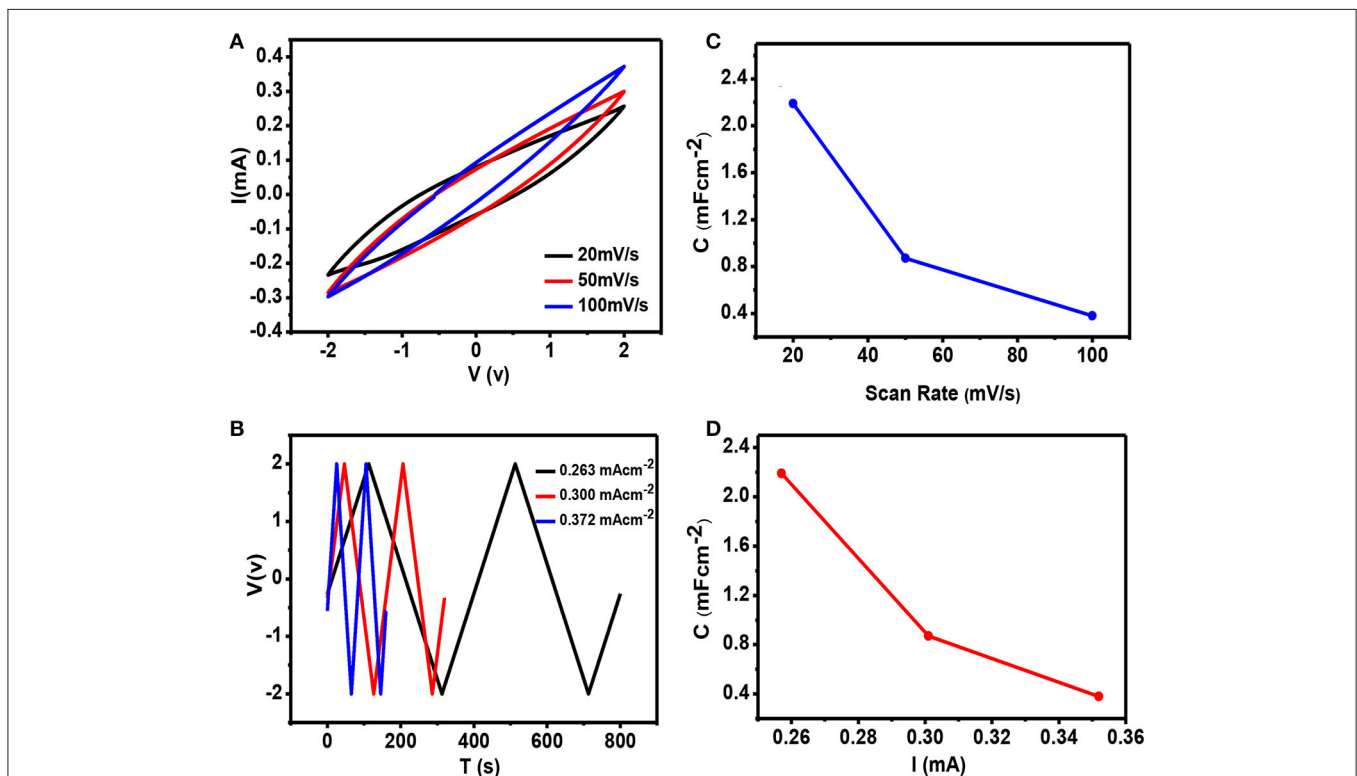


**FIGURE 6** | (A) Cyclic voltammety for the supercapacitor containing Iono-gel at scan rate of 20 mV/s, 50 mV/s and 100 mV/s at the potential window of  $-2$  to  $2$  V. (B) Charging and discharging curves of the supercapacitor. (C) Decreasing behavior of capacitance at different scan rates and at (D) capacitance and energy density analysis of the proposed device.

are produced in the region 600 to 1,400  $\text{cm}^{-1}$ . In IR spectra, the C = O bond stretching is produced from region 1,680 to 1,750  $\text{cm}^{-1}$ . While comparing both PI and LRPI C-N-C bonds, the reduction in the LRPI peak shows that some rearrangement has taken place. FTIR results confirms the carbon atoms that make the 3D structure of the LRPI layer result mainly from the rearrangement of carbonyl, phenyl ether and amide bonds from the carbon aromatic rings of the polyimide sheet.

So, the change in FTIR spectra of PI and LRPI material clearly shows that the bond structure of PI has changed, which resulted in the formation of the LRPI structure.

The electrochemical properties of the developed electrodes were tested in two electrode configurations using Iono-gel electrolyte (Cao et al., 2012). The utilization of the ionic electrolyte provides the advantage of using a wider voltage window, which in turn improves the overall energy density of the SC device. Thus, the assembled SC device was tested in a voltage window of  $\sim 2$  to 2 V. The CV analysis revealed a symmetric CV curve without any visible distortion, indicating charge storage through double layer formation as shown in **Figure 6**. The LRPI exhibited a high capacitance value of 2.19  $\text{mFcm}^{-2}$  at a scan rate of 20 mV/s. Moreover, no significant change in CV curve was observed upon increase in scan rate, indicating fast electrolyte diffusion through electrode materials (Mahmood et al., 2018a). The operation at large scan rate was enabled by presence of large channels in the carbon electrode which allow fast mass diffusion at higher scan rates (Mahmood et al., 2018b). Upon an increase in scan rate, capacitance of 0.87 and 0.38  $\text{mFcm}^{-2}$  is obtained at scan rates of 50 and 100 mV/s, respectively. The Galvanostatic charge/discharge curves were obtained to gain more insights into charge storage mechanism. As shown in **Figure 6**, the LRPI exhibited symmetric charge/discharge curves, which further confirms charge storage by double layer formation. Furthermore, an excellent relevance was observed between charging and discharging time, clearly indicating that the device has excellent Coulombic efficiency. Much similar to capacitance values obtained using CV analysis, the capacitance values calculated using Galvanostatic charge/discharge curves also exhibited a capacitance value of 2.19  $\text{mFcm}^{-2}$  at the scan rate of 20 mV/s. The energy density and power densities are calculated from Equations (3) and (4), respectively. The energy density of an LRPI-based SC device was found to be  $\sim 1.2167 \mu\text{Whcm}^{-2}$  at a corresponding power density of  $\sim 21.90 \mu\text{Wcm}^{-2}$ . It can be concluded that LRPI-based electrodes containing Iono-gel as electrolyte, not only increase the capacitance of the device but also increase the ionic conductivity of the SCs. This increase

in the capacitance is attributed to a 3D network of laser-induced graphene, showing that a higher surface area and having abundant wrinkles facilitates the diffusion of electrolytes for the formation of the Helmholtz layer.

## CONCLUSION

In summary, we reported the fabrication of SCs based on laser reduced polyimide material as electrodes. Fabrication of laser induced graphene electrodes have been made using a flexible polyimide sheet of 200  $\mu\text{m}$  thickness, using a computer-controlled semiconductor diode laser. The resulting reduced polyimide material has a large surface area, high porosity and high conductivity, which leads to numerous micro scale energy storage applications. After optimization, a fixed laser power of 164 mW was used for the fabrication of electrodes. This flexible SC reveals excellent electrochemical workings, for instance, high specific capacitance of 2.19  $\text{mFcm}^{-2}$  with a high energy density of 1.2167  $\mu\text{Whcm}^{-2}$ . Supercapacitors (SCs) are useful to future flexible electronics due to their comprising unique electrochemical properties, providing an approach for lightweight, cost effective, stretchable and flexible electrodes, which are an industrially-viable energy storage application.

## DATA AVAILABILITY STATEMENT

The original contributions presented in the study are included in the article/supplementary materials, further inquiries can be directed to the corresponding author/s.

## AUTHOR CONTRIBUTIONS

MA, ZK, SZ, and MAh adopted the concept, optimized the conditions, and fabricated the supercapacitor device. FN helped in characterization and synthesis of laser-reduced electrode. MI helped in synthesis of ionic liquids. AM helped in manuscript writing. MM, DA, and SR designed and supervised the whole project. All authors contributed to the article and approved the submitted version.

## ACKNOWLEDGMENTS

We are thankful to Higher Education Commission (HEC) of Pakistan and United States Agency for International Development (USAID) for providing research funding under the Project No. HEC/R&D/PAKUS/2017/783.

## REFERENCES

- Cao, Y., Xiao, L., Sushko, M., Wang, W., Schwenzer, B., and Xiao, J. (2012). Sodium ion insertion in hollow carbon nanowires for battery applications. *Nano Lett.* 7, 3783–3787. doi: 10.1021/nl3016957
- Faghih, K. H., and Ashouri, M. (2013). Synthesis and characterization of new polyimide/organoclay nanocomposites containing benzophenone moieties in the main Chain. *Chem. Soc.* 57, 133–136. doi: 10.29356/jmcs.v57i2.225
- Huang, G., Li, X., and Lou, L. (2018). Engineering bulk, layered, multicomponent nanostructures with high energy density. *Small* 11:1800619. doi: 10.1002/smll.201800619
- Hulicova, D., and Puziy, A. (2009). Highly stable performance of supercapacitors from phosphorus-enriched carbons. *Chem. Soc.* 131, 5026–5027. doi: 10.1021/ja809265m
- Lin, J., Peng, Z., and Liu, J. L. (2014). Laser-induced porous graphene films from commercial polymers. *Nat. Commun.* 5:6714. doi: 10.1038/ncomms6714

- Lin, J., Zhang, C., and Yan, Z. (2012). 3-Dimensional graphene carbon nanotube carpet-based microsupercapacitors with high electrochemical performance. *Nano letters*. 13, 72–78. doi: 10.1021/nl3034976
- Liu, J., Wang, L., and Braun, P. (2015). Mechanically and chemically robust sandwich-structured C@Si@C nanotube array Li-ion battery anodes. *ACS Nano*. 11, 1985–1994. doi: 10.1021/nn507003z
- Mahmood, A., Li, S., Zeehan, A., and Tabassum, H. (2018a). Ultrafast sodium/potassium-ion intercalation into hierarchically porous thin carbon shells. *Adv. Mater.* 31:1805430. doi: 10.1002/adma.201805430
- Mahmood, A., Tabassum, H., and Zhao, R. (2018b). Fe<sub>2</sub>N/S/N codecorated hierarchical porous carbon nanosheets for trifunctional electrocatalysis. *Small* 14:1803500. doi: 10.1002/smll.201803500
- Mahmood, A., Zou, R., and Wang, Q. (2016). Nanostructured electrode materials derived from metal-organic framework xerogels for high-energy-density asymmetric supercapacitor. *ACS Appl. Mater. Interfaces* 8, 2148–2157. doi: 10.1021/acsami.5b10725
- Mahmood, N., Tahir, M., and Mahmood, A. (2015). Hybrid of Co<sub>3</sub>Sn<sub>2</sub>@Co nanoparticles and nitrogen-doped graphene as a lithium ion battery anode. *Nano Energy* 11, 10307–10318. doi: 10.1021/nn4047138
- Malik, T., Naveed, S., and Munir, M. (2018). Fabrication and characterization of laser scribed supercapacitor based on polyimide for energy storage. *Adv. Mater.* 778, 181–186. doi: 10.4028/www.scientific.net/KEM.778.181
- Rathinam, K., Singh, S. P., Li, Y., Kasher, R., Tour, J. M., and Arnusch, C. J. (2017). Polyimide derived laser-induced graphene as adsorbent for cationic and anionic dyes. *Carbon N. Y.* 124, 515–524. doi: 10.1016/j.carbon.2017.08.079
- Romero, F., Salinas, A., Rivadeneyra, A., and Albrecht, A. (2018). In-depth study of laser diode ablation of kapton polyimide for flexible conductive substrates. *Nanomaterials*. 8:517. doi: 10.3390/nano8070517
- Tabassum, H., Mahmood, A., Wang, Q., and Xia, W. (2017). Hierarchical cobalt hydroxide and b/N Co-doped graphene nanohybrids derived from metal-organic frameworks for high energy density asymmetric supercapacitors. *Sci. Rep.* 7:43084. doi: 10.1038/srep43084
- Tabassum, H., Qu, C., and Cai, K. (2018). Large-scale fabrication of BCN nanotube architecture entangled on a three-dimensional carbon skeleton for energy storage. *Mater. Chem.* 6, 21225–21230. doi: 10.1039/C8TA08590K
- Winter, M., and Brodd, R. J. (2009). What are batteries, fuel cells, and supercapacitors? *Chem. Rev.* 104, 4245–4270. doi: 10.1021/cr020730k
- Xin, X., Ito, K., and Kubo, M. (2017). Efficient Br<sup>-</sup>/NO<sub>3</sub><sup>-</sup> dual-anion electrolyte for suppressing charging instabilities of Li–O<sub>2</sub> highly batteries. *ACS Appl. Mater. Interfaces* 9, 25976–25984. doi: 10.1021/acsami.7b05692
- Zhu, Y., Murali, S., Stoller, M., Ganesh, K., and Cai, W. (2011). Carbon-based supercapacitors produced by activation of graphene. *Science* 332, 1537–1541. doi: 10.1126/science.1200770

**Conflict of Interest:** The authors declare that the research was conducted in the absence of any commercial or financial relationships that could be construed as a potential conflict of interest.

Copyright © 2020 Asghar, Zahra, Khan, Ahmed, Nasir, Iqbal, Mohammad, Mahmood, Akinwande and Rizwan. This is an open-access article distributed under the terms of the Creative Commons Attribution License (CC BY). The use, distribution or reproduction in other forums is permitted, provided the original author(s) and the copyright owner(s) are credited and that the original publication in this journal is cited, in accordance with accepted academic practice. No use, distribution or reproduction is permitted which does not comply with these terms.